High-frequency electron paramagnetic resonance of the hole-trapped antisite bismuth center in photorefractive bismuth sillenite crystals

Ijaz Ahmad,[1] Vera Marinova,[1,2] and Etienne Goovaerts[1,*]

[1]*Department of Physics, Experimental Condensed Matter Physics, University of Antwerp, Universiteitsplein 1, B-2610 Antwerpen, Belgium*

[2]*Central Laboratory of Optical Storage and Processing of Information, Bulgarian Academy of Sciences, 1784 Sofia, Bulgaria*

(Received 9 October 2008; revised manuscript received 6 December 2008; published 26 January 2009)

The hole-trapped antisite bismuth center has been directly observed by *W*-band (94 GHz) electron paramagnetic resonance (EPR) in the series of sillenite crystals, $Bi_{12}MO_{20}$ (M=Ge, Si, Ti, denoted as BMO), either nondoped or doped with transition ions (Cr, Cu, Ru, Ce). Blue light illumination influences the EPR intensity in most crystals, while in nondoped $Bi_{12}GeO_{20}$ and $Bi_{12}SiO_{20}$ the signals only appear upon illumination. The spectra can be attributed to a single species and no anisotropy could be detected eliminating any significant deviation from tetrahedral symmetry due to a perturbing defect in the near neighborhood or to static lattice distortion. The large and isotropic hyperfine parameter, in good agreement with previous optically detected magnetic-resonance measurements [Phys. Rev. B **47**, 5638 (1993)], reveals that only ~25% of the hole is in the Bi $6s^1$ orbital, by delocalization mainly to the neighboring oxygen ions, with extremely small spin densities on the surrounding Bi^{3+} lattice ions as derived from the EPR linewidths. The parameter variations between the three crystalline hosts are very small, showing a near-identical degree of delocalization of the trapped hole.

DOI: 10.1103/PhysRevB.79.033107 PACS number(s): 73.20.Hb, 33.35.+r, 42.70.Nq

The photorefractivity of the sillenite type crystals $Bi_{12}MO_{20}$ (BMO) (where M=Si, Ge, or Ti) (Refs. 1–3) has been the subject of intensive research to understand and tailor the material properties for a range of applications such as multiwavelength holography,[4] real-time holographic surface imaging,[5] and holographic imaging and interferometry.[6] Crystalline defects (intrinsic or extrinsic) play an essential role for the magnitude, response time, and stability of the photorefractive (PR) effect. In conjunction with optical and electrical characterization techniques, electron paramagnetic resonance (EPR) has provided detailed information about the charge state and the microscopic structure of point defects and impurity centers involved in the optoelectronic properties, which has proven useful for the optimization of the properties of PR materials.[2,7] Sillenite crystals doped—either intentionally or not—with different impurities such as Fe, Mn, Ru, Rh, V, Cu, Co, Cr, Al, and Ga have been studied by EPR methods[8–11] and in particular by optically detected magnetic resonance (ODMR) (Refs. 11–14) which allows direct correlation of the paramagnetic defects with observed optical transitions.

In nondoped sillenite crystals, high-frequency ODMR (at ~94 GHz in the *W* band) allowed the study of a paramagnetic defect consisting of a hole trapped at an antisite Bi_M^{3+} center, i.e., a bismuth ion replacing a M^{4+} lattice ion with tetrahedral oxygen coordination.[15,16] This paramagnetic center, which we will somewhat loosely call the Bi_M^{4+} center, is produced by photoexcitation of an electron from the diamagnetic Bi_M^{3+} center to the conduction band after which it is trapped at other defect sites. This process is of major importance for the photorefractive properties of nondoped BMO crystals.[2,17,18] The diamagnetic Bi_M^{3+} center occurs in these crystals as a result of nonstoichiometry and is responsible for the tail in the optical absorption of these crystals,[19] which is the only absorption occurring below band-gap energy (~3.2 eV for the three BMO crystals) after proper (thermal or red light) initialization. Magnetic circular dichroism (MCD) and ODMR studies have shown that a composite photoinduced absorption band at lower energy is originating from the Bi_M^{4+} center. Here we present the first direct EPR measurements of the Bi_M^{4+} center in the three BMO sillenite hosts and discuss the influence of blue light illumination and of doping with various transition series ions on the production of the center. While confirming the analysis of the ODMR studies, the present EPR results allow us to critically reconsider the defect structures proposed in the literature.

Single crystals of $Bi_{12}SiO_{20}$ (BSO) and $Bi_{12}GeO_{20}$ (BGO) were grown in air from stoichiometric solution by the Czochralski method, while the $Bi_{12}TiO_{20}$ (BTO) crystals were obtained by the top seeded solution growth method, leading in each case to large crystals with high optical homogeneity. High purity oxides were used as starting materials, with dopants also in the form of oxides and platinum crucibles as containers. Further description of the growth procedures is provided in the articles in Ref. 20. Orientation of the single crystals was performed by x-ray diffraction (STOE four-circle diffractometer) in transmission through a thinned extremity of boule pieces. Using a thin diamond plate, bar-shaped pieces of suitable size to fit the *W*-band sample tubes (about 0.5 mm thick and 1.5 mm long) were cut with a long axis perpendicular to a (110) plane. The measurements were carried out in a continuous-wave *W*-band EPR spectrometer (Bruker Elexsys E680) operated at ~94.0 GHz and equipped with a continuous flow helium cryostat. Ar^+-ion laser light at 457 nm was used to illuminate the sample inside the cavity by means of an optical fiber threaded through the sample holder and ending at the top of the quartz sample tube.[21]

In Fig. 1, the EPR spectra measured at T=12 K in nondoped BSO are shown before and after several minutes of *in situ* illumination. Signals in the $g \cong 2$ region (at ~3.35 T) are present in both spectra, previously reported in *X*-band

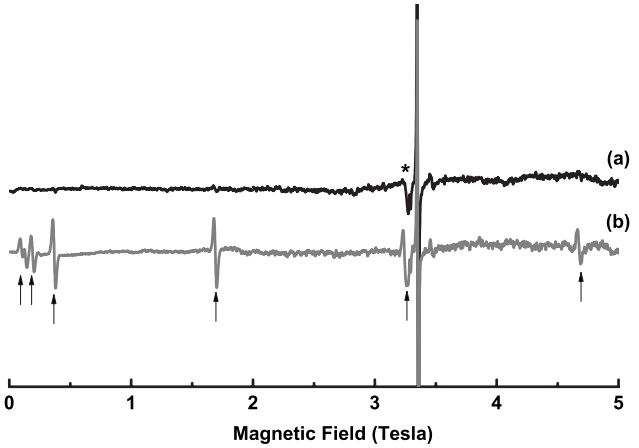

FIG. 1. *W*-band EPR spectrum of as-grown $Bi_{12}SO_{20}$ measured at 12 K (a) before illumination and (b) after 5–10 min exposure to 457 nm light. Arrows indicate the Bi_M^{4+} lines (a spurious cavity signal is marked ∗).

EPR studies[22–24] and attributed to intrinsic hole-trapped centers.[25] After 5–10 min of illumination a number of EPR resonances with relatively broad linewidth (~23 mT) appear over the whole field range [see Fig. 1(b)], which we identified with the Bi_M^{4+} center. This spectrum is not observed in room-temperature measurements. An angular study in the (110) plane shows that within experimental accuracy the EPR spectrum, including the low-field features, is perfectly isotropic, in agreement with tetrahedral symmetry. The four lines above 0.2 mT can be viewed as a set of near-equidistant lines with a splitting of ~1.5 T, part of the multiplet resulting from the very large isotropic hyperfine (hf) interaction with the ^{209}Bi nucleus (100% natural abundance, $I=9/2$). The latter follows from the partial localization of the hole in the 6*s* orbital of the Bi ion.[15] The same spectrum appears in doped BSO crystals (see, e.g., for Ru doping in Fig. 2) and near-identical spectra are found in BTO and BGO either nondoped or with various dopants [see, e.g., Fig. 3(a) for BTO:Cr]. The analysis was performed[26] using the spin Hamiltonian ($S=1/2$, $I=9/2$) adopted from Ref. 15,

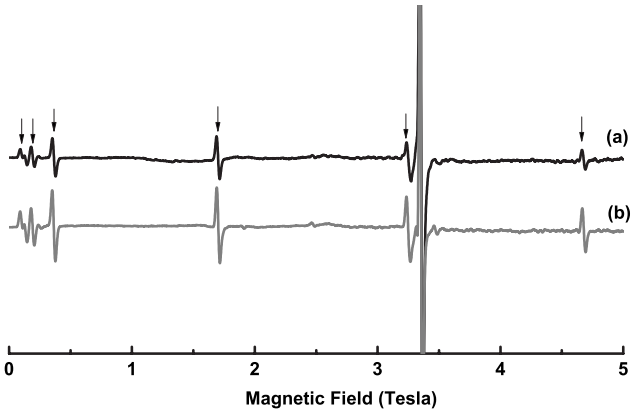

FIG. 2. *W*-band EPR spectrum of $Bi_{12}SO_{20}$:Ru measured at 12 K (a) before illumination and (b) after 5–10 min exposure to 457 nm light.

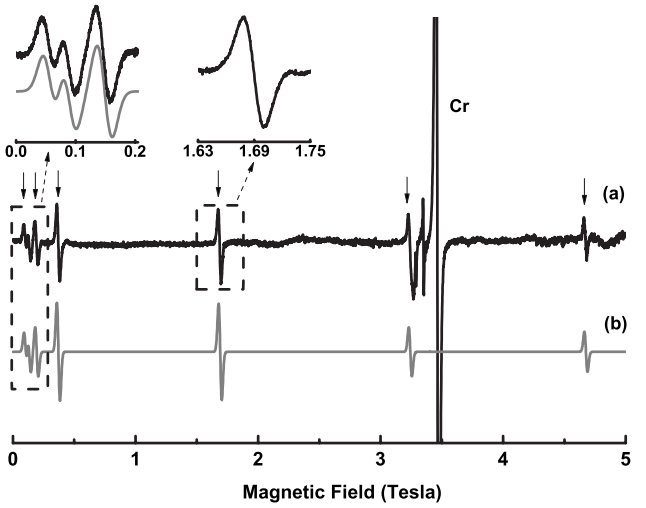

FIG. 3. *W*-band EPR spectrum of $Bi_{12}TiO_{20}$:Cr measured at 12 K (a) and plot (b) is the simulation of the Bi_M^{4+} spectrum with parameters of Table I. (Note the Cr-related signal.)

$$\boldsymbol{H} = g\boldsymbol{\mu}_B\boldsymbol{B}\cdot\boldsymbol{S} + A\boldsymbol{I}\cdot\boldsymbol{S}(-g_n\boldsymbol{\mu}_n\boldsymbol{B}\cdot\boldsymbol{I}), \quad (1)$$

with isotropic Zeeman and hf interactions (the nuclear Zeeman term is included for completeness but is found to be negligible in this analysis). The derived *g* and hf parameters are listed in Table I and a very good correspondence is obtained between simulated[27] and experimental spectra as shown for BTO in Fig. 3 (all line positions fit within 2 mT). Also in this table the parameters reported by Reyher *et al.*[15] are listed. Our more accurate hf parameter values fall within their experimental uncertainties. The *g* values are close to but slightly above the free-electron value, but there are significant discrepancies with the previous determination. Here, one should note that relatively few transitions could be identified and used for the analysis of the *W*-band ODMR spectrum,[15] which, moreover, were all lying in the low-field range (0.9–2.5 T), where the hf interaction is dominant. Our measurement of several high-field transitions definitely allows for a more reliable determination of the *g* parameter.

It should be noted that the EPR spectra of the Bi_M^{4+} center were found to be isotropic to very high accuracy and no indication is found for perturbation by other defects, e.g., vacancies, in the near neighborhood. For the isoelectronic ($6s^1$) ionic defects Tl^{2+} and Pb^{3+} in different ionic crystals, the effect of the low-symmetry environment is extensively documented.[28] There is no support for the existence of different variants of the Bi_M^{4+} center suggested[19] on the basis of the composite nature of the absorption spectrum. Symmetry lowering by lattice distortion was also invoked in Ref. 15 to explain a small nuclear quadrupole interaction introduced to explain discrepancies between *X*-, *Q*-, and *W*-band data and derivativelike features in the *W*-band ODMR spectra, but the EPR spectra do not show any effects of this kind.

EPR detection, contrary to ODMR, allows for measurements in the dark. In agreement with optical studies, no spectrum is detected in nondoped BSO and BGO crystals in their initial state (only doped BTO crystals were studied). Illumination in the violet (457 nm) produces the Bi_M^{4+} centers (see

TABLE I. The g and A parameters for the Bi_M^{4+} antisite defect in nondoped and doped BMO crystals compared to the ODMR results (between brackets) of Reyher *et al.* (Ref. 15).

Crystals	g	A (GHz)
BSO nondoped	2.0319 ± 0.0013 [2.049(5)]	19.332 ± 0.003 [19.35(6)]
BSO: Ru	2.0323 ± 0.0017	19.323 ± 0.004
BSO: Ce	2.0335 ± 0.0019	19.334 ± 0.005
BTO: Cr	2.0338 ± 0.0014 [2.05(1)]	19.334 ± 0.004 [19.2(1)]
BGO nondoped	2.0325 ± 0.0023 [2.041(3)]	19.224 ± 0.008 [19.21(5)]

Fig. 1) by excitation of an electron from the Bi_M^{3+} level to the conduction band. The studied BSO:Ce crystal followed essentially the same behavior as nondoped BSO, showing no specific donor or acceptor behavior for this impurity. In other doped crystals, BSO:Ru, BSO:Cu, BTO:Cr, and BTO:Ru, the hole-trapped center is already present in various amounts prior to illumination (see Fig. 3), indicating that mainly acceptor-type centers are induced by these dopants lowering the Fermi level and decreasing the electron occupation of the antisite bismuth centers. In all of these cases there is a significant increase in the Bi_M^{4+} concentration with illumination (Fig. 3) showing that there is an equilibrium between the two charge states which can be altered by optical excitation. Finally, in BSO codoped with Cr and P, no Bi_M^{4+} spectrum could be detected either before or after illumination. This could be related to a pronounced donor character of the dopants, but alternatively the concentration of antisite bismuth ions may be strongly decreased by the doping procedure, as previously demonstrated for several dopants in these BMO hosts.[18,19]

The g and A parameters for the Bi_M^{4+} center are the same for the three crystalline hosts within a very small margin, hardly outside of the experimental uncertainties, in good agreement with the ODMR results.[15] This would point to a very localized state for the trapped hole. However, the A values correspond to only an occupation of ~25% of the 6s orbital,[15] as was derived from comparison with calculated values[29] of the hf interaction in atomic bismuth, $A_{6s}=77$ GHz. (A case of localization near 50%, with $A=36.02$ GHz, has been reported[30] for Bi^{4+} in $CsAsF_6$.) In the present case, up to ~75% of the hole is thought to be spread over the surrounding ions, which are the four nearest-neighbor O^{2-} forming a tetrahedron and around them shells of substitutional Bi^{3+} ions. If some degree of delocalization over the bismuth neighbors is assumed, this should lead to an unresolved hf broadening of the EPR lines due to spin density in the 6s orbital of these ions. The observed peak-to-peak linewidth of ~23 mT, or equivalently ~63 MHz, also taking into account the high spin multiplicity for $I=9/2$, sets a level of the order of only ~0.1% to the spin density on the substitutional Bi neighbors. From this one can derive a picture of the Bi_M^{4+} center in which the hole is highly localized on the antisite bismuth ion and its four oxygen neighbors forming a BiO_4^{4-} molecular ion embedded in the crystal. In combination with the high structural similarity between the three crystals and lattice constants differing by less than 0.8%, this explains the near independence of EPR parameters on the host crystal.

Finally, it is worth considering the small-polaron model for this hole-trapped antisite defect as described by Schirmer,[31] involving the preferential localization of the hole onto one of the four oxygen ligands (i.e., a preferential bond between the bismuth ion and one of the oxygen neighbors). This would be averaged to tetrahedral symmetry by fast motion of the hole (and bond) between the four equivalent oxygen ions, probably by a tunneling motion since it is not freezing out down to our lowest measuring temperature ($T=5$ K). Since no motional effects occur in the EPR spectra, we could not further substantiate this model. This, however, sets a lower limit to tunneling frequency, which can be estimated to be $\nu_t \cong 2$ GHz.[32] This is compatible with an interpretation of the structure in the absorption spectrum, ascribing the splitting of $\Delta_{opt} \cong 0.3$ eV between two subbands at 2.6 eV to the trigonal distortion,[31] setting an upper limit $\nu_t \cong 70$ THz (Ref. 32) that is orders of magnitude higher than the lower bound from EPR. It is interesting to recall that this defect model was originally derived from a detailed study of ultrasonic attenuation in nondoped and doped BMO crystals.[33] A trigonal defect symmetry was derived with a thermally activated hopping between equivalent distortions. From the attempt frequencies and activation energies reported in this work, the hopping rate is reaching the megahertz range only above 25 K and thus static axial spectra would be expected in EPR at lower temperature. As previously stated, we do not find in EPR any sign of slowing down of vibronic dynamics, even at $T=5$ K. Therefore, the hole-trapped antisite defect studied in W-band ODMR and EPR cannot be identified with the one responsible for the ultrasound attenuation anomaly.

Financial support from FWO (Fund for Scientific Research, Flanders, Belgium) under Group Project No. G.0116.06N is kindly acknowledged. V.M. thanks the FWO for financial support during a postdoctoral visit. We are grateful to the Crystal Growth Laboratory of the Institute of Solid State Physics, Sofia, Bulgaria for the growth of the single crystals, supported by the Bulgarian National Fund under Project No. TK-X-1715/07.

*Corresponding author. etienne.goovaerts@ua.ac.be

[1] K. Buse, Appl. Phys. B: Lasers Opt. **64**, 391 (1997).
[2] B. Briat, V. G. Grachev, G. I. Malovichko, O. F. Schirmer, and M. Wöhlecke, in *Photorefractive Materials and Their Applications*, edited by P. Günter and J.-P. Huignard (Springer-Verlag, Berlin, 2007), Vol. 2, pp. 9–49.
[3] M. P. Petrov and V. V. Bryskin, in *Photorefractive Materials and Their Applications*, edited by P. Günter and J.-P. Huignard (Springer-Verlag, Berlin, 2007), Vol. 2, pp. 285–325.
[4] E. A. Barbosa, R. Verzini, and J. F. Carvalho, Opt. Commun. **263**, 189 (2006).
[5] M. R. R. Gesualdi, D. Soga, and M. Muramatsu, Opt. Laser Technol. **39**, 98 (2007).
[6] E. A. Barbosa, A. O. Preto, D. M. Silva, J. F. Carvalho, and N. I. Morimoto, Opt. Commun. **281**, 408 (2008).
[7] E. Possenriede, P. Jacobs, and O. F. Schirmer, J. Phys.: Condens. Matter **4**, 4719 (1992).
[8] H. J. von Bardeleben, J. Phys. D **16**, 29 (1983).
[9] V. Chevrier, J. M. Dance, J. C. Launay, and R. Berger, J. Mater. Sci. Lett. **15**, 363 (1996).
[10] N. K. Porwal, R. M. Kadam, Y. Babu, M. D. Sastry, M. D. Aggarwall, and P. Venkateswarlu, Pramana, J. Phys. **48**, 929 (1997).
[11] F. Ramaz, L. Rakitina, M. Gospodinov, and B. Briat, Opt. Mater. (Amsterdam, Neth.) **27**, 1547 (2005).
[12] B. Briat, A. Hamri, F. Ramaz, and H. Bou Rjeily, Proc. SPIE **3178**, 160 (1997).
[13] B. Briat, V. G. Grachev, G. I. Malovichko, O. F. Schirmer, and M. Wöhlecke, in *Photorefractive Materials and Their Applications*, edited by P. Günter and J.-P. Huignard (Springer-Verlag, Berlin, 2007), Vol. 2, pp. 36 and 37, and references therein.
[14] B. Briat, M. T. Borowiec, H. Bou Rjeily, F. Ramaz, A. Hamri, and H. Szymczak, Radiat. Eff. Defects Solids **157**, 989 (2002).
[15] H. J. Reyher, U. Hellwig, and O. Thiemann, Phys. Rev. B **47**, 5638 (1993).
[16] B. Briat, H. J. Reyher, A. Hamri, N. G. Romanov, J. C. Launay, and F. Ramaz, J. Phys.: Condens. Matter **7**, 6951 (1995).
[17] R. Oberschmid, Phys. Status Solidi A **89**, 263 (1985).
[18] B. C. Grabmaier and R. Oberschmid, Phys. Status Solidi A **96**, 199 (1986).
[19] H. Marquet, M. Tapiero, J. C. Merle, J. P. Zielinger, and J. C. Launay, Opt. Mater. (Amsterdam, Neth.) **11**, 53 (1998).
[20] M. Gospodinov and D. Petrova, Cryst. Res. Technol. **29**, 603 (1994); M. Gospodinov, S. Hausuhll, A. Sampil, and S. Dobreva, Mater. Res. Bull. **27**, 1415 (1992).
[21] G. Janssen, A. Bouwen, P. Casteels, and E. Goovaerts, Rev. Sci. Instrum. **72**, 4295 (2001).
[22] A. P. Eliseev, V. A. Nadolinnyi, and V. A. Gusev, J. Struct. Chem. **23**, 484 (1982).
[23] J. A. Baquedano, F. J. Lopez, and J. M. Cabrera, Solid State Commun. **72**, 233 (1989).
[24] E. Moya and C. Zaldo, J. Phys.: Condens. Matter **4**, L287 (1992).
[25] Attribution of $g \sim 2$ signals in vanadium doped BTO to the Bi_M^{4+} defect (also described as $Bi_M^{3+}+h^+$) as put forward by J. F. Carvalho, R. W. A. Franco, C. J. Magon, L. A. O. Nunes, F. Pellegrini, and A. C. Hernandes, Opt. Mater. (Amsterdam, Neth.) **13**, 333 (1999); Mater. Res. **2**, 87 (1999) is in contradiction with the results in Ref. 15 and in this work. It is in particular incompatible with the very large bismuth hf interaction.
[26] J. Glerup and H. Weihe, Acta Chem. Scand. **45**, 444 (1991).
[27] S. Stoll and A. Schweiger, J. Magn. Reson. **178**, 42 (2006).
[28] S. V. Nistor, D. Schoemaker, and I. Ursu, Phys. Status Solidi B **185**, 9 (1994); see pp. 49–57 and 65–66.
[29] J. R. Morton and K. F. Preston, J. Magn. Reson. (1969-1992) **30**, 577 (1978).
[30] A. R. Boate, J. R. Morton, and K. F. Preston, J. Chem. Phys. **67**, 4302 (1977).
[31] O. F. Schirmer, J. Phys.: Condens. Matter **18**, R667 (2006); see pp. R691–R692; see also B. Briat, V. G. Grachev, G. I. Malovichko, O. F. Schirmer, and M. Wöhlecke, in *Photorefractive Materials and Their Applications*, edited by P. Günter and J.-P. Huignard (Springer-Verlag, Berlin, 2007), Vol. 2, p. 33.
[32] Lower bound estimated from EPR: taking the isotropic g value as an average from an axial tensor with $g_\parallel = g_e$ (g_e: the free-electron g value) leads to an anisotropy $g_\perp - g_\parallel \cong 0.046$ and a characteristic frequency $(g_\parallel - g_\perp)\mu_B B/h$. Upper bound estimated from optical splitting: Δ_{opt}/h, with $\Delta_{\mathrm{opt}} \cong 0.3$ eV.
[33] W. Rehwald, K. Frick, G. K. Lang, and E. Meier, J. Appl. Phys. **47**, 1292 (1976); P. K. Grewal and M. J. Lea, J. Phys. C **16**, 247 (1983).